PAPER

Check for updates

Nanofibrous artificial skin substitute composed of mPEG–PCL grafted gelatin/hyaluronan/chondroitin sulfate/sericin for 2nd degree burn care: *in vitro* and *in vivo* study†

Sirsendu Bhowmick, [iD] ‡[abc] A. V. Thanusha,§[bc] Arun Kumar,§[bc] Dieter Scharnweber,[a] Sandra Rother[a] and Veena Koul [iD] *[bc]

The aim of this study was to investigate the efficacy of a skin substitute composed of mPEG–PCL–grafted-gelatin (Bio-Syn)/hyaluronan/chondroitin sulfate/sericin and to study its *in vitro* biocompatibility with human fibroblasts, human keratinocytes and hMSCs in terms of cellular adhesion and proliferation (∼5–6 fold). mPEG–PCL was grafted into a gelatin backbone *via* a Michael addition reaction to prepare Bio-Syn and it was characterized using ATR-FTIR, ^{1}H NMR and TNBS assay. Additionally, keratinocyte–hMSC contact co-culture studies showed that Bio-Syn composite scaffolds loaded with sericin promote hMSCs' epithelial differentiation with regard to qRT-PCR gene expression (ΔNp63α and keratin 14) and expression of various epithelial markers (Pan-cytokeratin, ΔNp63α and keratin 14). *In vivo* efficacy studies on a 2nd degree burn wound model in Wistar rats showed an improved rate of wound contraction, histology (H&E and Van Gieson's staining) and pro-healing marker (hexosamine, hydroxyproline, *etc.*) expression in granular tissue compared to using the commercial dressing Neuskin™ and a cotton gauze control.

Background

Advances in many aspects of burn wound healing have led to improvements in the survival rate of burn victims. Consequently, deaths because of burns have decreased to half in the last four decades.[1] Regardless of the developments in burn wound healing, secondary infection, delayed healing and mobility are still complex problems that need to be addressed.[2] A skin wound initiates a series of actions, including inflammation, remodeling and proliferation.[3] Since the last decade, the design and development of ideal scaffolds to heal injured tissues has been the key focus in the area of tissue engineering and biomaterials. Scaffolds with explicit functions and uses, like reduced scar formation, reduced risk of microbial infection

and biological relevance, are a developing field in this area.[4] Scientists have used different techniques to prepare 3D scaffold frameworks to increase pore interconnection and porosity.[5]

Recently, electrospinning has grown in reputation in the field of tissue engineering as a method to form prospective scaffolds for tissue regeneration purposes (soft tissue and blood vessels).[4] Scientists have used several synthetic, biological or biological–synthetic polymers, *viz.* (a) elastin–collagen, (b) gelatin–hyaluronan, (c) biocomposites of poly(ether-ether-ketone)/-hydroxyapatite, and (d) chitosan based polymers, to fabricate fibrous scaffolds and they witnessed improved *in vitro* cellular proliferation.[6,7] Applications of biopolymers for scaffold preparation are restricted due to their faster degradation and poor mechanical properties, while scaffolds prepared using synthetic polymers lack RGD motifs, which are essential for cellular attachment.[5,8] This study assessed bio-synthetic (hybrid) polymeric composite scaffolds composed of methoxypolyethyleneglycol (mPEG)–polycaprolactone (PCL)–grafted-gelatin (Bio-Syn: mPEG–PCL–*g*-Gelatin), sericin, hyaluronan (HA) and chondroitin sulfate (CS), imitating the cellular microenvironment for the dermal tissue healing process. Gelatin (partially hydrolyzed collagen) is used here as the backbone of the bio-hybrid polymer *i.e.* mPEG–PCL is grafted into a gelatin backbone to prepare the bio-hybrid polymer (Bio-Syn) and to improve the mechanical properties and degradation behavior of the scaffold. Gelatin's usage for scaffold fabrication

^{a}Max-Bergmann Center of Biomaterials Dresden, Technische Universität Dresden, Budapester Straße 27, 01069, Dresden, Germany

^{b}Centre for Biomedical Engineering, Indian Institute of Technology Delhi, Hauz Khas, New Delhi 110016, India. E-mail: veenak@iitd.ac.in; veenak_iitd@yahoo.com; Tel: +91-11-26591041; +91-11-26596187

^{c}Biomedical Engineering Unit, All India Institute of Medical Sciences, New Delhi 110029, India

† Electronic supplementary information (ESI) available. See DOI: 10.1039/c8ra01489b

‡ Current address: Department of Chemistry, University at Albany, State University of New York, Albany, New York 12222, United States. Email: sbhowmick@albany.edu, sirsendu.tito@gmail.com. Tel: +1-518-442-4412.

§ These authors contributed equally to this work.

is well known as its RGD motif supports cellular adhesion.[9] Chen *et al.* prepared a poly(lactic acid) electrospun scaffold modified with cationic gelatin for cartilage tissue engineering purposes.[10] Glycosaminoglycans (GAGs) are anionic polysaccharide molecules that play a crucial part in helping different stages of skin tissue maturation and development, regardless of them being a minor constituent of dermal ECM. GAGs interact with different proteins, including various cytokines and growth factors, and modulate their activity.[4,11] Chang *et al.* prepared a hyaluronan/chondroitin/gelatin scaffold for cartilage tissue engineering and observed promotion in ECM secretion (including type II collagen), while cultivating porcine chondrocytes.[12] Previously, our group studied the *in vivo* and *in vitro* efficacy of a gelatin electrospun scaffold loaded with epigallocatechin gallate (EGCG) for excisional wounds and observed faster degradation behavior (6 days)[13] compared to a designed Bio-Syn composite scaffold.

The biochemical microenvironment of cells and the intercellular interactions between different adult cells play a vital role in the dermal tissue development and maturation process.[4,14,15] The ability of multipotent mesenchymal stem cells (MSCs) to differentiate towards different mesenchymal lineages, *viz.* osteogenic, chondrogenic or adipogenic roots, is well known.[16] There are also indications of differentiation of MSCs down endodermal, neuroectodermal and mesodermal lineages *via* intercellular interaction with adult cells *i.e. in vitro* coculture models.[17] However, there are always arguments between researchers about whether such incidences are true differentiation or just events of cell fusion.[4,17] Sivamani *et al.* showed that MSCs can differentiate towards early neural lineages and myofibroblasts while cultured without the proximity of keratinocytes, whereas they differentiate down the epithelial linage during direct contact co-culture of keratinocyte–hMSC.[17] We have previously reported that a cationic gelatin composite electrospun scaffold and keratinocyte–hMSC contact co-culture has synergistically improved the epithelial marker expression in hMSCs.[4]

According to the literature review and our previous findings,[4] here we investigated a greatly improved scaffold system, a sericin loaded Bio-Syn composite scaffold fabricated by mixing mPEG–PCL–*g*-gelatin (Bio-Syn)/HA/CS for dermal wound healing purposes. mPEG–PCL–*g*-gelatin (Bio-Syn) was used here as a base material and HA/CS/sericin was used as a bioactive component, mimicking the cell microenvironment to design electrospun scaffolds, which might be used for burn and trauma care. The *in vitro* efficacy of the scaffolds was evaluated on monocultures of human keratinocytes (HaCaT), fibroblasts (Hs27) and mesenchymal stem cells (hMSCs) by means of cellular adhesion and proliferation, and then the influence on epithelial differentiation of hMSCs in a keratinocyte–hMSC co-culture model was studied. The *in vivo* efficiency of the scaffold was examined on a 2nd degree burn wound model in Wistar rats in terms of wound contraction, histology (H&E stain and Van Gieson's stain) and pro-healing marker expression in granular tissue in comparison with the commercial dressing Neuskin™ and a cotton gauze control.

Materials and methods

The materials and methods are described in the ESI.†

Results

Characterization of Bio-Syn

The reaction scheme for mPEG–PCL grafted gelatin is shown in Fig. 1. In the first step, the di-block copolymer (mPEG–PCL–OH) was synthesized *via* ε-caprolactone ring opening polymerization using mPEG as an initiator in the presence of the catalyst tin(ɪɪ)2-ethylhexanoate. The ^{1}H NMR and ATR-FTIR spectra confirmed the successful synthesis of the mPEG–PCL di-block copolymer (ESI Fig. S1 and S2†). As per the ^{1}H NMR spectra, the characteristic peaks at δ 1.35–1.43, 1.60–1.70, 2.28–2.32 and 4.03–4.08 represent the methylene units of polycaprolactone. The peak at δ 3.64 corresponds to the methylene units of mPEG, confirming the synthesis of the di-block polymer. The FTIR spectra also confirmed the synthesis of the di-block copolymer by the ester (–C=O) stretching vibration bands at 1721.70 cm^{-1}, the asymmetric –C–H stretching vibration bands at 2943.92 cm^{-1} and the symmetric –CH stretching vibration bands at 2860 cm^{-1}. Additionally, the C–H binding vibration bands at 1366.21 cm^{-1}, the –C–C– stretching vibration bands at 1470.98 cm^{-1} and the ether (–O–) stretching vibration bands at 1105.65 cm^{-1} also demonstrate the synthesis of the di-block copolymer. The molecular weight of the di-block copolymer was evaluated using ^{1}H NMR and GPC. According to the ^{1}H NMR results, the molecular weight of the di-block copolymer was 4109 Da, whereas using GPC, M_n and M_w were 3250 Da and 6590 Da (Fig. S3†), respectively.

In the second step, the terminal hydroxyl (–OH) of the di-block copolymer was modified to an acryloyl group (–COCH=CH$_2$) by reacting it with acryloyl chloride in the presence of triethyl amine. The product was characterized using ATR-FTIR and ^{1}H NMR spectra. According to the ^{1}H NMR spectra, there is one new multiplet peak in the range δ 5.71–5.633 that corresponds to the acryloyl group, confirming the synthesis of the acryloyl modified di-block copolymer (mPEG–PCL–O–CO–CH=CH$_2$). The FTIR spectra of gelatin was characterized using the following absorption bands: the –OH stretching vibration bands at 3288.73 cm^{-1}, the –C–H stretching vibration bands at 2929.57 cm^{-1} and the amide (–NH–CO–) stretching vibration bands at 1630.87 cm^{-1}.

In the final step, the synthetic di-block copolymer was grafted into the gelatin backbone *via* a Michael addition reaction. The product was characterized using ATR-FTIR and ^{1}H NMR spectra. As per the ^{1}H NMR spectra, the multiplet broad peaks at δ 1.43 and 1.50 are because of the merging of peaks at δ 1.35–1.43 of mPEG–PCL–OH and δ 0.850/1.22 of gelatin, and δ 1.60–1.70 of mPEG–PCL–OH and δ 1.54–2.01 of gelatin. Additionally, the multiplet broad peak responsible for CH=CH$_2$ at δ 5.71–5.633 disappeared from the spectra, confirming successful grafting of the di-block copolymer into the gelatin backbone. mPEG–PCL grafting into the gelatin backbone was confirmed by the presence of stretching vibration bands at 3306.66 cm^{-1} (–OH stretching of gelatin), 2943.84 cm^{-1} (asymmetric –C–H stretching of mPEG–PCL), 2860 cm^{-1} (symmetric –C–H
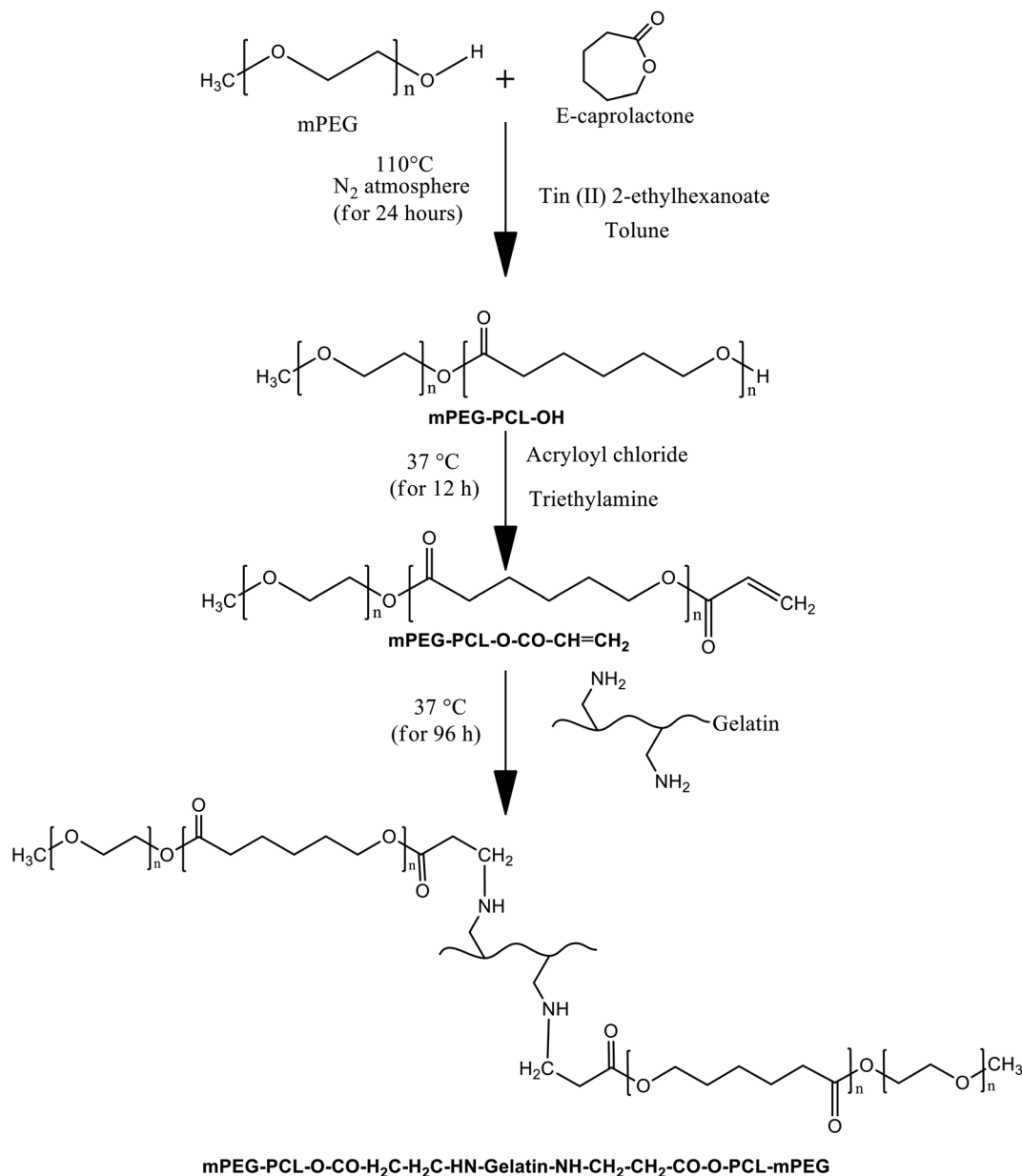
Fig. 1 Reaction scheme for the synthesis of the Bio-Syn polymer (mPEG–PCL–g-gelatin).

stretching of mPEG–PCL), 1721.85 cm^{-1} (ester (–C=O) stretching of mPEG–PCL) and 1643.33 cm^{-1} (amide (–NH–CO–) stretching of gelatin). The degree of substitution was evaluated using TNBS assay and found to be 13 ± 2%.

Evaluation of the Bio-Syn electrospun nanofibrous composite scaffold

The microscopically electrospun scaffold was studied using a scanning electron microscope (SEM) (Fig. 2A and B) to observe the fiber morphology. A mean fiber diameter of 193 ± 49 nm was observed throughout the scaffold. However, the fiber morphology in terms of shape and size was not altered by varying the concentration of sericin. A histogram of the fiber diameter is shown in Fig. 2C.

The scaffolds' porosity was evaluated using a porometer *via* the method of liquid extrusion. The porosity percentage (89.38 ± 1.9%) and mean pore size (0.96 ± 0.1 μm) were observed while exposing the scaffolds to 12.27 ± 0.77 PSI negative pressure. No statistically significant difference in the fiber porosity was observed by changing the sericin concentration.

In terms of the mechanical properties, the maximum force at break (MF) and the Young's modulus (YM) increased by 95.76% and 85.3%, respectively in the case of the sericin loaded Bio-Syn composite scaffold compared to that of the native Bio-Syn composite scaffold. However, after GTA crosslinking, a drastic increment (**$p < 0.01$) was observed in both YM (1772%) and MF (1387%) in the sericin loaded Bio-Syn composite scaffold compared to the native Bio-Syn composite scaffold.
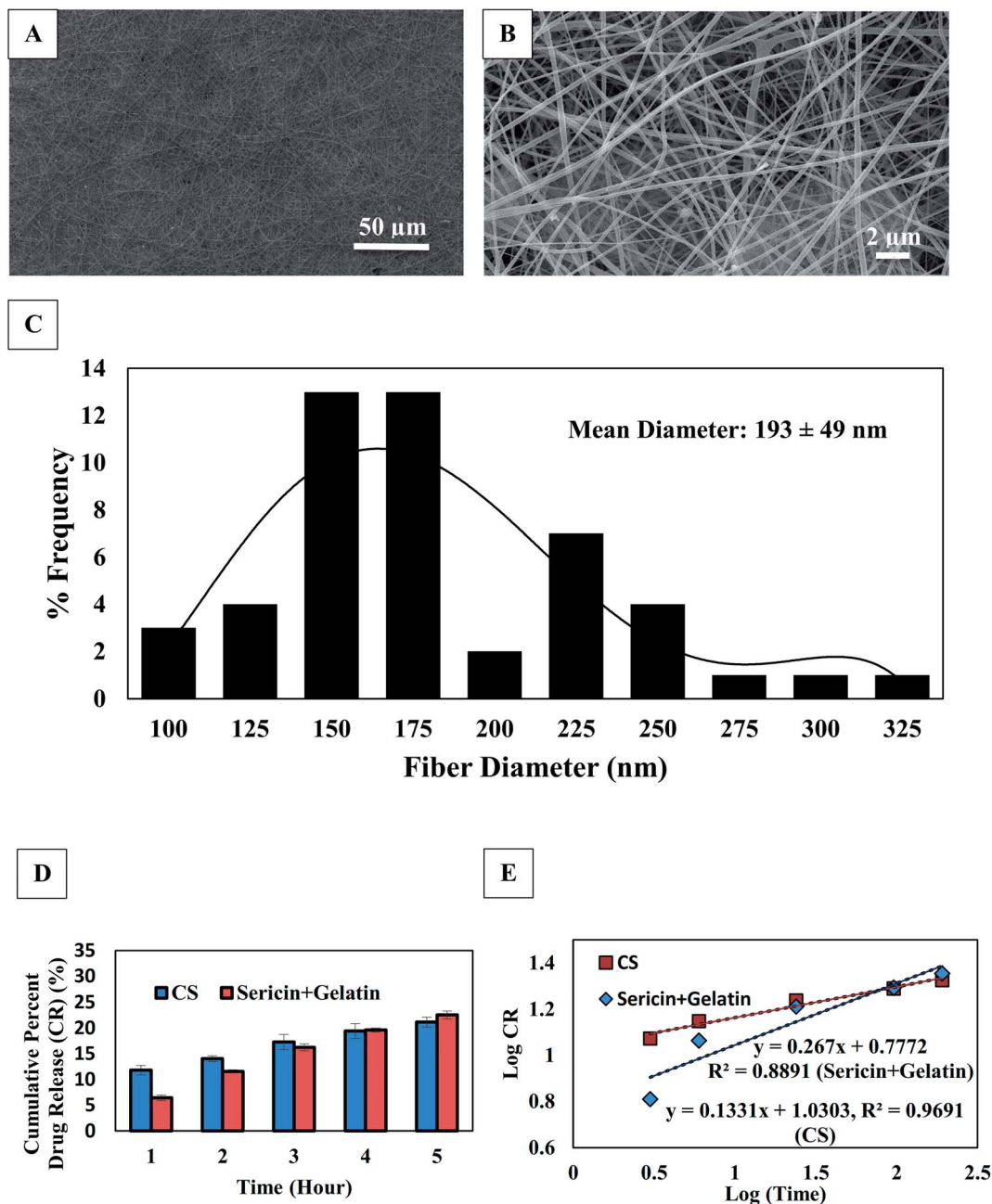
Fig. 2 Evaluation of 1% sericin loaded Bio–Syn composite scaffold; (A) fiber morphology observed under SEM at 1000× magnification, (B) fiber morphology observed under SEM at 10 000× magnification, (C) histogram plot of fiber diameter in SEM micrograph, (D) protein (sericin/gelatin) and CS release behavior in PBS and (E) release kinetics of protein (sericin/gelatin) and CS.

It was not possible to evaluate the degradation behavior of the Bio–Syn composite scaffold *via* a conventional gravimetric method because of the gentle nature of the wetted Bio–Syn composite scaffold. So the degradation study was performed using the Lowry protein assay.[18] The native scaffold was firm for 63 days, however the 1% sericin loaded Bio–Syn composite scaffold lasted for 65 days in a solution of PBS. At day 8, ~10% and ~8% weight loss was observed, but ~21% and 15% loss of weight was found on day 32, in the cases of the native scaffold and the 1% sericin Bio–Syn composite scaffold, respectively.

The scaffolds were stained with toluidin blue[19] to examine the distribution of sulfated GAGs. Microscopically, it was witnessed that the scaffolds were stained blue (CS), showing evenly distributed CS all over the scaffold. Additionally, the existence of GAGs (CS/HA) was further confirmed *via* gel electrophoresis (1% agarose) as per the method described by Rother *et al.*[20]

Fig. 2D shows the release profile of CS and proteins from the scaffold. According to the Korsmeyer–Peppas model, the main drug release mechanism is Fickian diffusion when the diffusion exponent value (n) $\leq$ 0.5. Anomalous transport (when 0.5 < n $\leq$

1.0; diffusion plus erosion) is generally characterized by non-Fickian release. n is calculated from the slope of $\log_{10}(f)$ versus $\log_{10}(t)$ (Fig. 2E). The linearity was calculated from the graphical plot of $\log$(drug release) versus $\log$(time). The release kinetics of CS and proteins were examined from the exponent (n) and it was observed that the CS and the protein (sericin/gelatin) coefficient values (n) were 0.133 and 0.267, respectively. Hence, the chief release mechanism of CS and proteins is predicted to be diffusion.

Cellular proliferation on the Bio-Syn composite scaffold – biochemical analysis

The interaction of cell–matrix–cell plays a vital role in cellular migration and granular tissue contraction into the wound bed.[21] Adhesion and proliferation of the cells was examined on a control collagen coated coverslip and sericin loaded Bio-Syn composite scaffolds. Around ~20 000 cells were seeded into each scaffold and kept in a CO_2 incubator for 2 hours for initial cellular adhesion and the number of initial adhered cells was evaluated using LDH and Pico Green DNA quantification assays [Hs27 (14 807 ± 697), HaCaT (15 723 ± 561) and hMSCs (15 129 ± 756)]. About 75% initial adhesion efficiency was observed independent of sericin presence.

Similar cellular growth behavior was witnessed for all cells and scaffolds in terms of both DNA quantification and the LDH assay (Fig. 3). The keratinocyte (HaCaT) and fibroblast (Hs27) cell numbers doubled from day 1 to day 3. The same phenomenon was observed for hMSCs from day 7 to day 14. In summary, cellular proliferation was observed while cultivating cells of the sericin loaded Bio-Syn composite scaffold. This was dependent on the presence of GAGs as well as the concentration of sericin. The Bio-Syn composite scaffold loaded with 1% sericin showed the highest cell proliferation for all cell types at day 3 or day 14, respectively.

Cellular proliferation on the Bio-Syn composite scaffold – immunofluorescence imaging

Scaffolds were stained using Phalloidin Alexa Fluor 564 and DAPI to examine the influence of the scaffold on cellular proliferation. Because of the autofluorescent nature of gelatin, high autofluorescence was observed in all samples. The findings of Li et al. also line up with the above observations.[7,22] It was observed that on all scaffolds, fibroblasts, keratinocytes and hMSCs adhered and proliferated (Fig. 3G). It was observed microscopically that the cellular density on the scaffold increased with an increasing concentration of sericin.

Contact co-culture of keratinocyte–hMSCs on the Bio-Syn composite scaffold

After co-culturing for 5 days, a sub-population of hMSCs attained a keratinocyte-like shape and started expressing epithelial markers e.g. pan-cytokeratin, ΔNp63α and keratin 14 (K14), while a different sub-population acquired fibroblast-like morphology. Some of the hMSCs that started expressing epithelial protein markers contained multiple nuclei, while others had a single nucleus. This phenomenon of transdifferentiation in adult stem cells might be because of cellular fusion, which is predominant in co-culture models.[23–25] hMSCs containing multiple nuclei in contact co-culture similarly indicate transdifferentiation (cellular fusion) instead of true differentiation. The scaffold with 1% sericin showed a relatively higher level of epithelial protein expression in the truly differentiated hMSCs compared to that in the native Bio-Syn composite scaffold. Because of the high confluency of the keratinocytes in the scaffold, the images were taken primarily at the edge of the scaffold to avoid high fluorescence and to identify truly differentiated non-fused hMSCs from the sub-population of contact co-culture (Fig. 4, 5C & S4†).

FACS and gene expression analysis – keratinocytes–hMSCs contact co-cultivation model on the Bio-Syn composite scaffold

To nullify the controversies regarding cellular fusion and to evaluate the true differentiation of hMSCs down the epithelial lineage, flow-cytometry was used to collect the mono-nucleated hMSCs (non-fused) from the co-culture of keratinocyte–hMSC as per the procedure explained by Sivamani et al.[17] (Fig. 5A). FACS data suggested that the majority of hMSCs were fused with neighboring keratinocytes, however there was not much proof of cellular fusion in the immunofluorescence images as they were acquired at the edge of the scaffold to avoid high fluorescence from confluent keratinocytes. Fused cells isolated from FACS were examined microscopically to confirm the cellular fusion. As mentioned in an earlier section, FACS isolated non-fused hMSCs were observed for keratinocyte marker expression (ΔNp63α and K14) and exhibited upregulation in gene expression compared to the control hMSCs (Fig. 5B), signifying differentiation down the epithelial lineage.

FACS analysis for co-culture study on the 1% sericin loaded Bio-Syn composite scaffold is shown in Fig. 5A. FACS results revealed that the majority of hMSCs (1.31%) were found to be fused with neighboring keratinocytes (Fig. 5). In four quadrant gating, (a) the keratinocytes stained blue were represented in the Q1 quadrant, (b) the fused double stained cells were represented in the Q2 quadrant, (c) hMSCs stained green were represented in the Q3 quadrant and (d) the unstained cells were represented in the Q4 quadrant. The gene expression level of ΔNp63α and K14 was evaluated using mRNA transcript with qRT-PCR (Fig. 5B). A significant increase in both of the gene expressions was observed compared to the control, however no statistical significance was found among different scaffold groups.

In vivo evaluation of the Bio-Syn composite scaffold in Wistar rats

Wound contraction. Fig. 6A & S5† show photographs of the burn wound on days 0, 7, 14 and 21, while Fig. 6B displays the wound contracted area after the application of the Bio-Syn composite scaffold on days 7, 14 and 21. On day 0, the wound area was ~95.07 mm^2 (11 mm diameter) in all groups. The rate of wound contraction with the Bio-Syn composite scaffold loaded with 1% sericin (55.21 ± 1.85 mm^2, 21.87 ± 2.03 mm^2,
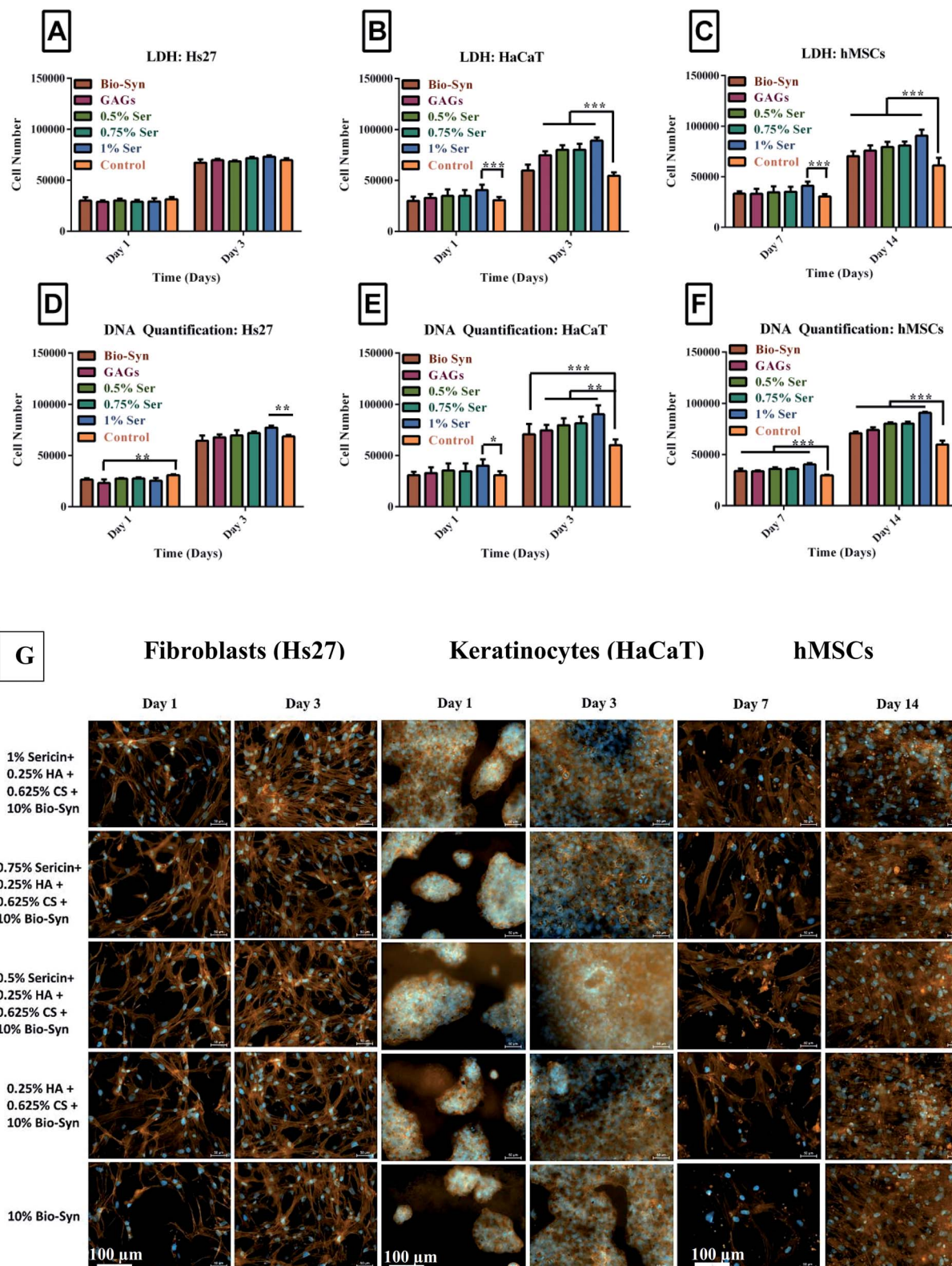
Fig. 3 Cellular proliferation shown by LDH assay on (A) Hs27 cells, (B) HaCaT cells, and (C) hMSCs; and by Pico Green dsDNA quantification assay on (D) Hs27 cells, (E) HaCaT cells, and (F) hMSCs. (G) Fibroblast, keratinocyte and hMSC cultured Bio-Syn scaffolds were immunostained (red-orange) at the cytoskeleton with Alexa Fluor 564 Phalloidin and at the nucleus (blue) with DAPI. The 10% Bio-Syn composite scaffold served as a control. The data presented in this figure are in terms of the mean ± SD. In this figure, the abbreviations used are (i) Bio-Syn: 10% Bio-Syn composite scaffold, (ii) GAGs: 0.25% HA + 0.625% CS + 10% Bio-Syn, (iii) 0.5% Ser: 0.5% sericin + 0.25% HA + 0.625% CS + 10% Bio-Syn, (iv) Ser: 0.75% sericin + 0.25% HA + 0.625% CS + 10% Bio-Syn and (v) 1% Ser: 1% sericin + 0.25% HA + 0.625% CS + 10% Bio-Syn. 10 mm coverslips coated with collagen were examined as a control. ($n = 8$); *$p < 0.05$, **$p < 0.01$, ***$p < 0.001$ scaffold groups.
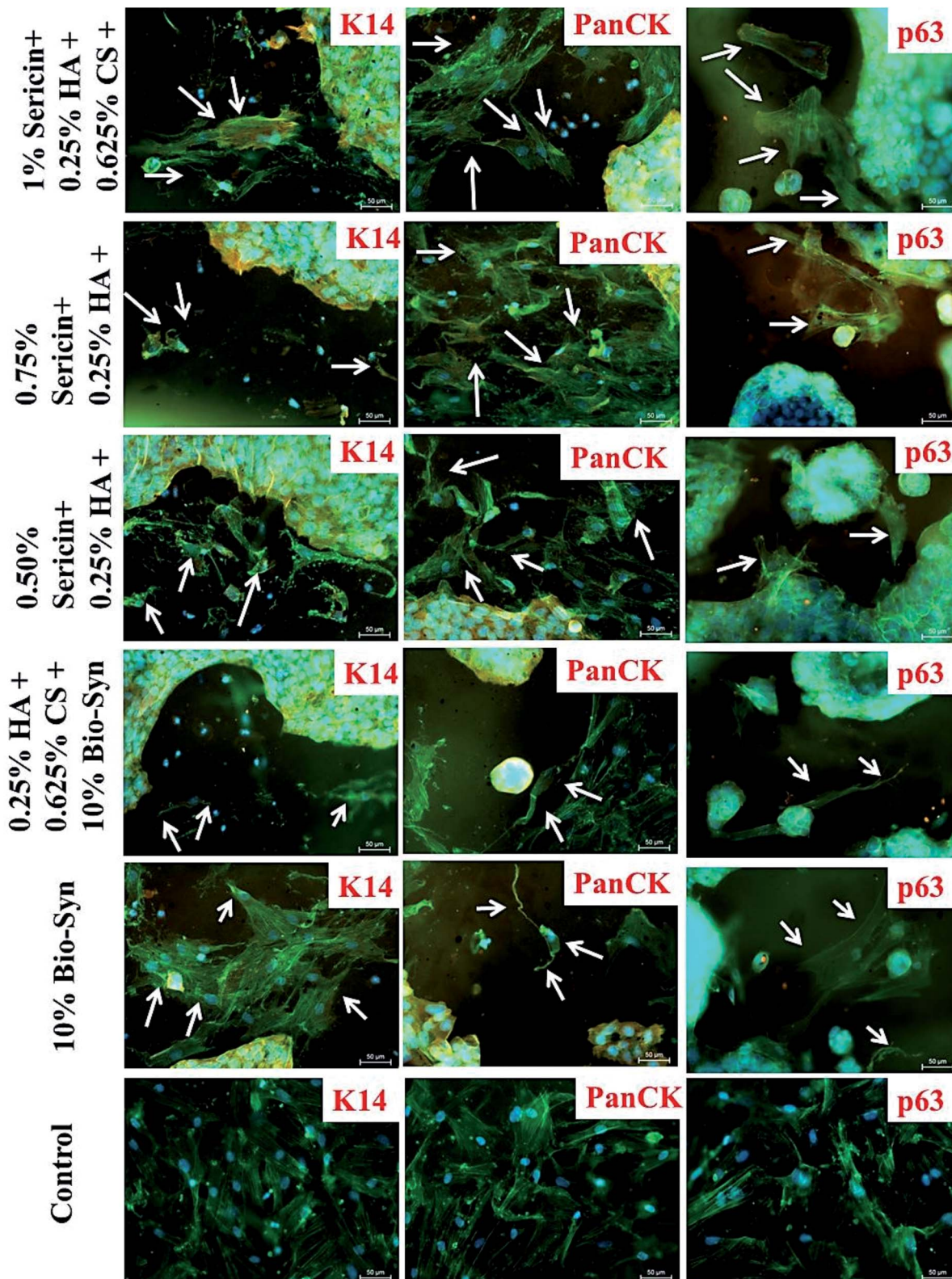
Fig. 4   After 5 days of contact co-culture, the scaffolds were immunostained (color: red-orange) using Keratin 14 (K14), Np63α (p63), and Pan-cytokeratin (PanCK) monoclonal antibody, Phalloidin Alexa Fluor 488 (color: green) and DAPI (color: blue). The white arrows point towards epithelial differentiated hMSCs in the co-culture sub-population.
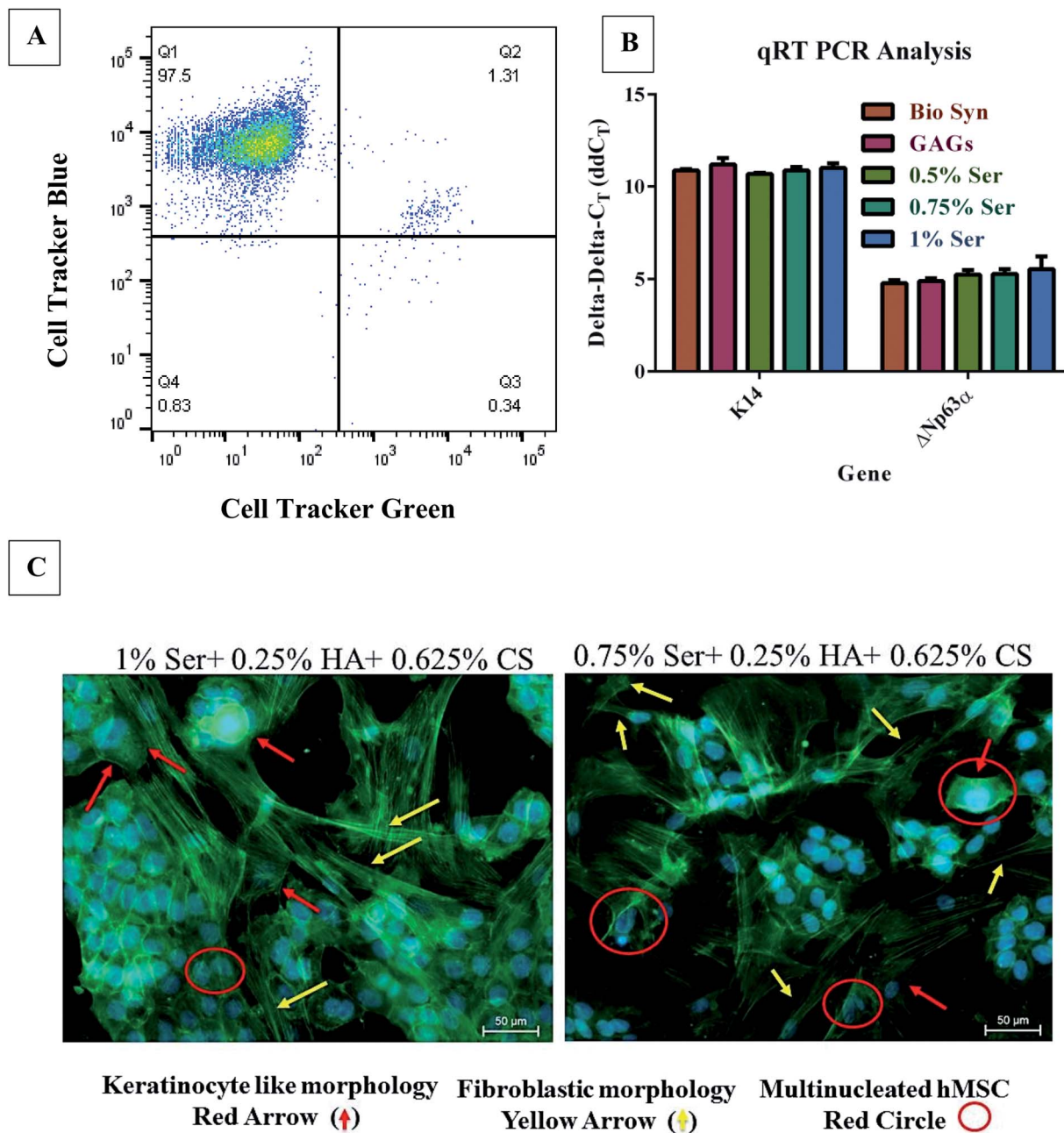
Fig. 5 Keratinocyte–hMSC co-cultivation on the 1% sericin loaded Bio-Syn composite scaffold. (A) Four quadrant gated FACS analysis of keratinocyte (CTB)–hMSC (CTG) contact co-cultured. (B) Keratin 14 and Np63α gene-expression analysis was assessed using qRT-PCR with mRNA transcript in a co-culture model of keratinocyte–hMSCs. hMSCs cultivated alone on the respective scaffold were used as the control. (C) A hMSC sub-population acquired a round keratinocyte-like morphology (red arrow), whereas another sub-population became stretched and attained a fibroblast-like shape (yellow arrow), liberated from the Bio-Syn composite scaffold type. During co-culture, multinucleated cells (red circle) were also witnessed. hMSCs cultivated on 10% Bio-Syn composite scaffolds were considered as the control. Data are represented here in terms of the mean ± SD. ($n = 3$).

and 0.79 ± 0.45 mm^2) was observed to be significantly superior compared to that with the commercial dressing Neuskin™ (60.57 ± 1.79 mm^2, 30.07 ± 2.33 mm^2, and 1.37 ± 0.59 mm^2) and cotton gauze (69.21 ± 2.96 mm^2, 35.53 ± 4.81 mm^2, and 1.22 ± 0.67 mm^2) on days 7, 14 and 21, respectively.

Biochemical and histological evaluation. Dermal tissue samples were collected on days 7, 14 and 21 for examining the

pro-healing markers, as described in Table 1. The Bio-Syn composite scaffold loaded with 1% sericin showed improvement in all biochemical parameters in comparison with the commercial dressing Neuskin™ and the cotton gauze control (Table 1).

Fig. 6C shows a histological micrograph of H&E stained dermal tissue samples on days 7, 14 and 21 at 10×
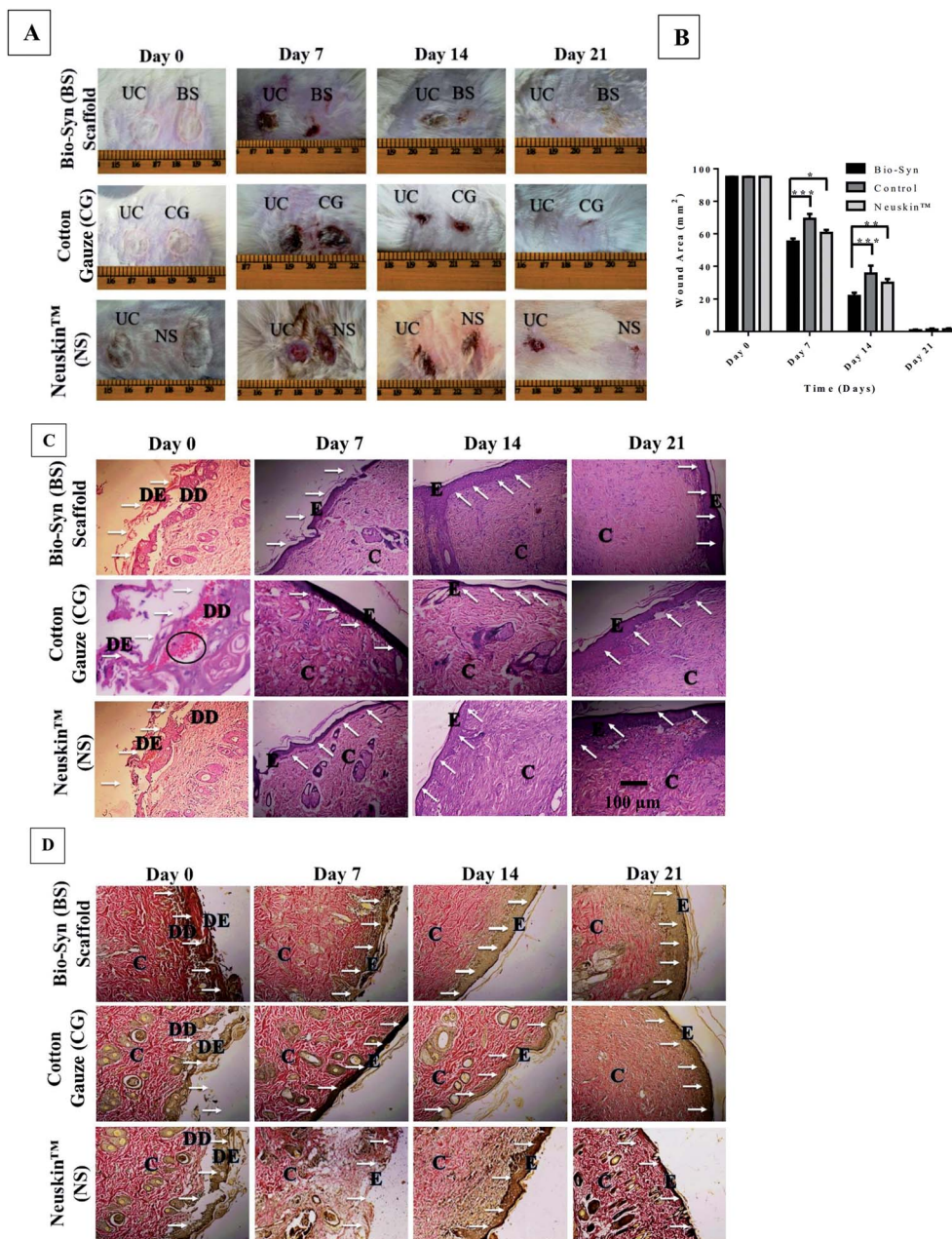
Fig. 6 (A) Representative photographs for 2nd degree burn wounds at days 0, 7, 14 and 21, (B) wound contraction area of wound tissue in the Bio-Syn, cotton gauze and Neuskin™ groups at days 0, 7, 14 and 21. The data are represented as the mean ± SD; $n = 6$ rats, (C) H&E stained histological section of wound tissue in the Bio-Syn, cotton gauze and Neuskin™ groups at days 0, 7, 14 and 21 (10× magnification), (D) Van Gieson's (VG) stained histological section of wound tissue in the Bio-Syn, cotton gauze and Neuskin™ groups at days 0, 7, 14 and 21. The collagen stain is bright red, while the cytoplasm, muscle and fibrin stain is yellow. The white arrows indicate the epidermal healing process, while the black circles indicate ruptured blood capillaries. Abbreviations used in these images: "UC" untreated control, "DE" dead epidermis, "DD" dead dermis, "E" epidermis and "C" collagen fiber.

magnification. Necrosis and neutrophil (polymorphonuclear leukocytes [PMN]) infiltration on vascular and surface tissue in the wound area was observed in images of the H&E stained skin tissue samples of the control groups (Neuskin™ and cotton gauze), whereas the deeper zone of the wound bed showed new collagen formation and fibroblast proliferation at day 7. While examining the wound bed superficial zone, necrotic tissue and pronounced infiltration of PMN were observed below and on

top, respectively. At day 14, a thin layer of newly formed epidermis was observed in the control group, while at day 21 the damaged epidermis and dermis portion were almost completely healed and new collagen fiber was observed in the deeper part of the skin.

The animal group treated with the 1% sericin loaded Bio-Syn composite showed approximately 75% re-epithelization on the surface tissue in the wound bed at day 7 and day 14 compared to

Table 1 Evaluation of biochemical parameters and pro-healing markers in the Bio-Syn composite scaffold, commercial dressing (Neuskin™) and cotton gauze control treated groups. Data are presented as mean ± SD; $n = 6$ (for Neuskin™: $*p < 0.05$, $**p < 0.01$, $***p < 0.001$) (for cotton gauze: $\#p < 0.05$, $\#\#p < 0.01$, $\#\#\#p < 0.001$) (mg g^{-1} of dry tissue weight)/(mg of dry tissue weight). (+++) represents the maximum response while (−) refers to the minimum response

	Bio-Syn composite scaffold			Cotton gauze control			Neuskin™		
Parameter	Day 7	Day 14	Day 21	Day 7	Day 14	Day 21	Day 7	Day 14	Day 21
DNA (mg g^{-1})	2.8 ± 0.1$^{\#\#}$	4.02 ± 0.3$^{\#}$	4.35 ± 0.2$^{\#\#}$	1.7 ± 0.37	2.56 ± 0.4	3.95 ± 0.5	2.1 ± 0.6	3.68 ± 0.2	4.25 ± 0.4
Protein (mg g^{-1})	133 ± 2.1$^{\#\#\#}$	152 ± 3.7$^{\#\#\#}$	165 ± 4.2	92.2 ± 1.36	137 ± 3	156 ± 5.6	129.6 ± 2.3	146 ± 1.5	158 ± 1.7
HAE (mg g^{-1})	0.9 ± 0.02$^{***,\#\#\#}$	1.1 ± 0.05$^{***,\#\#\#}$	1.14 ± 0.03$^{\#}$	0.53 ± 0.07	0.89 ± 0.04	1.05 ± 0.04	0.59 ± 0.02	0.96 ± 0.04	1.09 ± 0.08
HP (mg g^{-1})	47 ± 3.23$^{**,\#\#}$	62 ± 4.93$^{*,\#}$	84 ± 3.7$^{\#}$	32.9 ± 3.03	49 ± 4.21	77 ± 2.1	35.07 ± 3.6	47 ± 5.1	78 ± 1.8
Acute inflammation	±	±	−	+++	++	±	+	++	−
Chronic inflammation	±	±	−	++	+	±	+	+	−
Edema	+	−	−	+++	+	+	+	+	−
Granular tissue formation	++	+++	+++	++	+	+	++	+	+
Collagen formation	++	+++	++	+	++	+	+	++	++
Re-epithelization	++	+++	+++	±	+	++	−	+	+

commercial dressing Neuskin™ and cotton gauze control, whereas a completely healed epidermis and dermis were witnessed at day 21. In the deeper part of the wound bed, noticeable collagen formation and fibroblast proliferation was observed along with a few blood vessels, whereas a thick epidermal layer on the top tissue with lower inflammatory response was observed in the superficial area of the wound.

It was also observed that the sericin loaded Bio-Syn composite scaffold elicited collagen and granular tissue formation, while edema and inflammatory response (monocytes and polymorphonuclear leukocytes) were reduced compared to the commercial dressing Neuskin™ and the cotton gauze control groups at day 14 and day 21. Furthermore, there was almost a negligible amount of inflammatory cells and re-epithelization was optimized in the sericin loaded composite scaffold, both of which are essential for faster wound healing and support the potential of the scaffold as artificial skin. Additionally, the skin tissue sample stained with VG collagen (Fig. 6D) showed matured and compact collagen formation with the sericin loaded Bio-Syn composite scaffold in comparison to that with the commercial dressing Neuskin™ and in the cotton gauze control group at day 14 and day 21. The collagen fibers were deposited in parallel to the epidermis layer, which indicates the maturity of the wounded tissue.

Discussion

In the case of wound healing, the prime requirement of a functionalized biomaterial is to assist the injured tissue *via* promoting the functionality of cells and improving the mechanism of healing.[26] Tissue–biomaterial interactions are generally governed by particular types of cell surface receptor. Therefore, the fundamental requirements of a biomaterial are to deliver an appropriate platform that supports cellular adhesion, proliferation and differentiation. As of yet, the methodologies of *in vitro* cell culture are still lacking the biophysical extracellular microenvironments

of dermal tissue, which is present during skin regeneration. Based on this background, the objective of this present work was to fabricate a bio-hybrid, biocompatible and biodegradable base that will not only promote cell proliferation but also stimulate the cell differentiation process, which is an essential factor for improved skin regeneration.

Evaluation of the Bio-Syn composite scaffold

Evenly distributed fibers with a diameter of 193 ± 49 nm were observed in the SEM micrograph of the electrospun scaffold. No change in fiber morphology was witnessed by varying sericin or GAG concentration. The findings of our previous work also line up with the above observation.[4,13] Additionally, Li *et al.* prepared electrospun scaffolds by blending gelatin and HA, and also found similar results.[27] The *in vitro* release study revealed that the primary release mechanism of CS and proteins (gelatin/sericin) is Fickian diffusion (Fig. 2E). After 192 h in PBS, 22.53 ± 0.76% and 21.15 ± 0.96% proteins and CS were released from the scaffold, respectively. Hempel *et al.* designed artificial ECM coatings *via in vitro* fibrillogenesis of collagen I and sulfated HA and observed initial sulfated GAG release of 25 μg.[28] However, the release stabilized (~12 μg) after 3 hours. In this study, we have observed a much slower and more sustained release of protein (3.69 ± 0.12 μg after 192 hours) and CS (2.85 ± 0.13 μg after 192 hours) from the sericin loaded Bio-Syn composite scaffold. The improved mechanical properties ($**p < 0.01$) of the sericin loaded Bio-Syn composite scaffold might be because of the interaction between GAGs, sericin and Bio-Syn as well as mPEG–PCL grafting into the gelatin backbone. The –COOH and –NH$_2$ groups of Bio-Syn might have interacted with GAGs and sericin and acted as a composite system *via* hydrogen bonds (non-covalent), leading to interruption of the movement of the polymer chain and consequently resulting in enhanced degradation, mechanical properties and sustained release. This is further supported by the findings obtained by our group (sericin

loaded composite scaffold and EGCG loaded gelatin nano-fibrous scaffold).[4,13]

Effects of the Bio-Syn composite scaffold on cellular behavior

Electrospun blends of Bio-Syn/CS/HA/sericin were used to prepare the defined artificial microenvironment, mimicking the composition and micro-structure of the natural ECM of dermal tissue. Independently of sericin and GAGs' presence, the Bio-Syn electrospun nanofibrous scaffold supports initial adhesion (after 2 h) in all three cell types. However, no significant difference (statistically) in cellular growth was witnessed among different scaffold types.

Migration and proliferation of fibroblasts and keratinocytes into the wound is the primary factor in skin wound healing.[29,30] Therefore, the *in vitro* biocompatibility of the scaffolds was examined on three types of skin lineage cell and significantly higher proliferation was observed while culturing for a longer time period (Fig. 3). van der Smissen *et al.* demonstrated similar findings of fibroblast proliferation on aECMs containing highly-sulfated GAGs.[31]

Proliferation, migration and maturation of hMSC towards the epithelial cells is a crucial aspect for dermal wound healing. Hanukoglu showed that activin A, which belongs to the family of TGF-β, stimulates K14 expression (K14 are proteins that belong to the family of keratin I)[32] and thereby stimulates dermal fibroblast proliferation, which therefore improves the process of wound healing.[33] It was observed during FACS analysis that a majority of the population of the hMSCs is multinucleated *i.e.* they became fused (multinucleated) with adjacent keratinocytes, liberated of the different scaffold types. However, another group of hMSCs that have non-fused cells (mono-nucleated) displayed improvement in K14 expression (Q2 of Fig. 5A) while co-cultured on the 1% sericin loaded Bio-Syn composite scaffold in comparison with that on the native Bio-Syn electrospun nanofibrous scaffold (Fig. 5B).

p63, a tumor suppressor gene[34,35] that is homologous to p53, expresses two major protein classes: (a) ΔNp63 and (b) TAp63. Expression of ΔNp63α plays a crucial role in modulating the migration and behavioral morphology of skin lineage cells.[17] In this study, ΔNp63α expression also increased on the Bio-Syn composite scaffold loaded with 1% sericin compared to that on the native scaffold (Fig. 5B). Evidence of the hMSCs' differentiation towards the epithelial lineage was also further confirmed by immunocytochemical imaging of epithelial markers (PanCK, K14 and p63). Additionally, it was also witnessed that an hMSC subgroup acquired fibroblast-like morphology (fibrous and elongated) while another subgroup acquired keratinocyte-like morphology and became spherical (Fig. 4, 5C and S4†). A similar phenomenon was also witnessed by Tucci *et al.* and Sivamani *et al.*[17,36]

Comparative analysis between the Bio-Syn composite scaffold and a cationic gelatin composite scaffold

We have previously reported the preparation, characterization and biological evaluation of a cationic gelatin composite scaffold[4] (Cat Gel) containing the same bioactive components (HA/CS/sericin). The base polymer, cationic gelatin, was prepared by grafting a quaternary ammonium group, whereas in the present study, we have synthesized a novel hybrid polymer by grafting mPEG–PCL (synthetic polymer) into a gelatin (biopolymer) backbone. In spite of the similar bioactive components in both scaffold systems (Cat Gel *vs.* Bio-Syn), here we observed a significant improvement in physical properties compared to the Cat Gel scaffold *viz.* (a) fiber diameter (206 ± 45 nm *vs.* 193 ± 49 nm), (b) porosity (0.57 ± 0.07 μm *vs.* 0.96 ± 0.1 μm), (c) improved mechanical properties, (d) degradation behavior (45 days *vs.* 65 days), and (e) release coefficient (proteins: 0.1402 *vs.* 0.133; GAGs: 0.095 *vs.* 0.267), respectively. In both cases, we observed similar cellular proliferation (∼5 fold) for all cell types (Hs27, HaCaT and hMSCs). However, while evaluating their influence in hMSC epithelial differentiation, we curiously observed that the Bio-Syn native polymer scaffold (without the bioactive components) showed a significant improvement in epithelial marker expression (K14: ∼9.9 fold; p63: ∼25 fold) compared to that of the native Cat Gel scaffold. Based on this comparative analysis, we may conclude that the grafting of the synthetic polymer into the gelatin backbone has not only improved its physical properties but also its biological behavior in a significant manner compared to that of the Cat Gel scaffold. The reason for the improvement in epithelial marker expression could be the presence of PEG–PCL in the scaffold, which possibly results in neutral behavior and thus reduces the charge of gelatin, providing better proliferation.

Influence of the Bio-Syn composite scaffold on burn wound healing

Improving skin tissue quality by stimulating dermal tissue functionality, and boosting the wound contraction rate, is the leading field in dermatological research and tissue engineering.[13] Hexosamine and hydroxyproline are generally used as biological markers for granulation tissue and collagen, respectively.[13] The mitotic potential of the wounded tissue can be assessed using the enhancement in DNA and protein content. The *in vivo* study showed an improved wound contraction rate in Wistar rats treated with the sericin loaded Bio-Syn composite scaffold compared to with the commercial dressing Neuskin™ and the cotton gauze control (Fig. S5†). Additionally, the histological evaluation of the collected skin tissue showed lower inflammatory response, and dense matured and parallel collagen on days 7, 14 and 21 on the sericin loaded Bio-Syn composite scaffold, while biochemical analysis revealed the upregulation of prohealing markers (protein, DNA, hydroxyproline, hexosamine), which incidentally support the improvement in the quality of healed burnt tissue. Covering the Bio-Syn composite scaffold with a semi-permeable cellophane membrane played a crucial role in maintaining a humid and moist environment in the wound bed for 7 days and indorsed gaseous exchange around the wound bed.

Based on the findings of the *in vitro* (DNA quantification, LDH assay, immunocytochemistry, and qRT-PCR) and *in vivo*

(wound contraction, histopathology and biochemical analysis for pro-healing markers) studies, we summarized that the Bio-Syn composite scaffold loaded with sericin promotes hMSCs' epithelial differentiation in a contact co-culture model of keratinocyte–hMSC and stimulates 2nd degree burn wound healing in Wistar rats due to cellular adhesion and growth of human mesenchymal stem cells, human keratinocytes and human fibroblasts, and thus it could be valuable for burn and trauma care.

Conclusion

In conclusion, this present work has revealed that both the extracellular microenvironment and intracellular interactions with the adjacent cells can improve the epithelial differentiation process of hMSCs while cultivating in proximity to keratinocyte on sericin loaded Bio-Syn composite scaffolds. Bio-Syn composite scaffolds with 1% sericin significantly boosted the wound healing process in a 2nd degree burn wound model on Wistar rats in terms of wound contraction and expression of pro-healing markers in granular tissue compared to the commercial dressing Neuskin™ and a cotton gauze control. The above findings suggest that the Bio-Syn composite scaffold loaded with sericin might act as an admirable dermal substitute for improved healing of 2nd degree burn wounds and can be used for clinical purposes in burn care.

Author contributions

S. B. designed the work and performed the experiments. A. K. assisted during the synthesis phase, A. V. T. assisted during the animal experiments and S. R. assisted during the cell culture work. D. S. and V. K. reviewed the article and supervised the project.

Conflicts of interest

The authors declare no competing financial interest.

Acknowledgements

References

1 N. F. Ribeiro, C. H. Heath, J. Kierath, S. Rea, M. Duncan-Smith and F. M. Wood, *Burns*, 2010, **36**, 9–22.
2 D. Church, S. Elsayed, O. Reid, B. Winston and R. Lindsay, *Clin. Microbiol. Rev.*, 2006, **19**, 403–434.
3 D. N. Heo, D. H. Yang, J. B. Lee, M. S. Bae, J. H. Kim, S. H. Moon, H. J. Chun, C. H. Kim, H.-N. Lim and I. K. Kwon, *J. Biomed. Nanotechnol.*, 2013, **9**, 511–515.
4 S. Bhowmick, D. Scharnweber and V. Koul, *Biomaterials*, 2016, **88**, 83–96.
5 R. V. Shevchenko, S. L. James and S. E. James, *J. R. Soc., Interface*, 2010, **7**, 229–258.
6 S. Bhowmick, S. Rother, V. Hintze, S. Möller, M. Schnabelrauch, V. Koul and D. Scharnweber, Electrospun Nanofibrous Scaffolds Composed of Gelatin and Sulfated Hyaluronan for Wound Healing Applications, *European Burn Association Congress 2015, Annals of Burns and Fire Disasters*, Supplement EBA, 2015, vol. 28, p. 42.
7 M. Li, Y. Guo, Y. Wei, A. G. MacDiarmid and P. I. Lelkes, *Biomaterials*, 2006, **27**, 2705–2715.
8 F. Groeber, M. Holeiter, M. Hampel, S. Hinderer and K. Schenke-Layland, *Adv. Drug Delivery Rev.*, 2011, **63**, 352–366.
9 E. Ruoslahti, *Annu. Rev. Cell Dev. Biol.*, 1996, **12**, 697–715.
10 J.-P. Chen and C.-H. Su, *Acta Biomater.*, 2011, **7**, 234–243.
11 C. I. Gama, S. E. Tully, N. Sotogaku, P. M. Clark, M. Rawat, N. Vaidehi, W. A. Goddard, A. Nishi and L. C. Hsieh-Wilson, *Nat. Chem. Biol.*, 2006, **2**, 467–473.
12 C.-H. Chang, H.-C. Liu, C.-C. Lin, C.-H. Chou and F.-H. Lin, *Biomaterials*, 2003, **24**, 4853–4858.
13 M. Jaiswal, A. Gupta, A. K. Agrawal, M. Jassal, A. K. Dinda and V. Koul, *J. Biomed. Nanotechnol.*, 2013, **9**, 1495–1508.
14 S. Bhowmick, S. Rother, H. Zimmermann, P. S. Lee, S. Moeller, M. Schnabelrauch, V. Koul, R. Jordan, V. Hintze and D. Scharnweber, *Mater. Sci. Eng. C*, 2017, **79**, 15–22.
15 S. Bhowmick, S. Rother, H. Zimmermann, P. S. Lee, S. Moeller, M. Schnabelrauch, V. Koul and D. Scharnweber, *J. Mater. Sci.: Mater. Med.*, 2017, **28**, 128.
16 A. I. Caplan, *J. Orthop. Res.*, 1991, **9**, 641–650.
17 R. K. Sivamani, M. P. Schwartz, K. S. Anseth and R. R. Isseroff, *FASEB J.*, 2011, **25**, 122–131.
18 O. H. Lowry, N. J. Rosebrough, A. L. Farr and R. J. Randall, *J. Biol. Chem.*, 1951, **193**, 265–275.
19 D. Terry, R. Chopra, J. Ovenden and T. Anastassiades, *Anal. Biochem.*, 2000, **285**, 211–219.
20 S. Rother, J. Salbach-Hirsch, S. Moeller, T. Seemann, M. Schnabelrauch, L. C. Hofbauer, V. Hintze and D. Scharnweber, *ACS Appl. Mater. Interfaces*, 2015, 23787–23797.
21 B. Hinz, *J. Invest. Dermatol.*, 2007, **127**, 526–537.
22 M. Li, M. J. Mondrinos, M. R. Gandhi, F. K. Ko, A. S. Weiss and P. I. Lelkes, *Biomaterials*, 2005, **26**, 5999–6008.
23 J. L. Spees, S. D. Olson, J. Ylostalo, P. J. Lynch, J. Smith, A. Perry, A. Peister, M. Y. Wang and D. J. Prockop, *Proc. Natl. Acad. Sci. U. S. A.*, 2003, **100**, 2397–2402.
24 N. Terada, T. Hamazaki, M. Oka, M. Hoki, D. M. Mastalerz, Y. Nakano, E. M. Meyer, L. Morel, B. E. Petersen and E. W. Scott, *Nature*, 2002, **416**, 542–545.
25 Q.-L. Ying, J. Nichols, E. P. Evans and A. G. Smith, *Nature*, 2002, **416**, 545–548.

26 D. F. Williams, *Biomaterials*, 2009, **30**, 5897–5909.

27 J. Li, A. He, C. C. Han, D. Fang, B. S. Hsiao and B. Chu, *Macromol. Rapid Commun.*, 2006, **27**, 114–120.

28 U. Hempel, V. Hintze, S. Möller, M. Schnabelrauch, D. Scharnweber and P. Dieter, *Acta Biomater.*, 2012, **8**, 659–666.

29 A. D. Metcalfe and M. W. Ferguson, *J. R. Soc., Interface*, 2007, **4**, 413–437.

30 A. D. Metcalfe and M. W. Ferguson, *Biomaterials*, 2007, **28**, 5100–5113.

31 A. van der Smissen, V. Hintze, D. Scharnweber, S. Moeller, M. Schnabelrauch, A. Majok, J. C. Simon and U. Anderegg, *Biomaterials*, 2011, **32**, 8938–8946.

32 I. Hanukoglu and E. Fuchs, *Cell*, 1982, **31**, 243–252.

33 B. Munz, H. Smola, F. Engelhardt, K. Bleuel, M. Brauchle, I. Lein, L. W. Evans, D. Huylebroeck, R. Balling and S. Werner, *EMBO J.*, 1999, **18**, 5205–5215.

34 A. Yang, M. Kaghad, Y. Wang, E. Gillett, M. D. Fleming, V. Dötsch, N. C. Andrews, D. Caput and F. McKeon, *Mol. Cell*, 1998, **2**, 305–316.

35 A. J. Levine, R. Tomasini, F. D. McKeon, T. W. Mak and G. Melino, *Nat. Rev. Mol. Cell Biol.*, 2011, **12**, 259–265.

36 P. Tucci, M. Agostini, F. Grespi, E. K. Markert, A. Terrinoni, K. H. Vousden, P. A. Muller, V. Dötsch, S. Kehrloesser and B. S. Sayan, *Proc. Natl. Acad. Sci. U. S. A.*, 2012, **109**, 15312–15317.